

THE TOPOLOGY OF HYDROGEN BONDING IN BRANDTITE, COLLINSITE AND FAIRFIELDITE

SASHA HERWIG AND FRANK C. HAWTHORNE[§]

Department of Geological Sciences, University of Manitoba, Winnipeg, Manitoba R3T 2N2, Canada

ABSTRACT

The crystal structures of brandtite $[\text{Ca}_2(\text{Mn,Mg})(\text{AsO}_4)_2(\text{H}_2\text{O})_2]$, monoclinic, a 5.877(1), b 12.957(2), c 5.675(1) Å, β 108.00(3)°, V 411.0 Å³, space group $P2_1/c$, $Z = 2$], collinsite $[\text{Ca}_2(\text{Mg,Fe})(\text{PO}_4)_2(\text{H}_2\text{O})_2]$, triclinic, a 5.729(1), b 6.778(1), c 5.444(1) Å, α 97.31(3), β 108.63(3), γ 107.25(3)°, V 189.8 Å³, space group $P1$, $Z = 1$] and fairfieldite $[\text{Ca}_2(\text{Mn,Mg})(\text{PO}_4)_2(\text{H}_2\text{O})_2]$, triclinic, a 5.795(1), b 6.576(1), c 5.495(1) Å, α 102.39(3), β 108.63(3), γ 90.29(3)°, V 194.0 Å³, space group $P1$, $Z = 1$] have been refined to R indices of 2.6, 1.5 and 1.7%, respectively, based on 1200, 1089 and 1137 unique $|F_o| > 5\sigma F$ reflections measured with an automated four-circle single-crystal X-ray diffractometer equipped with a serial detector and a MoK α X-ray source. The brandtite, collinsite and fairfieldite structures are based on infinite $[M(\text{TO}_4)_2(\text{H}_2\text{O})_2]$ chains parallel to the c axis and with a repeat distance of ~5.55 Å. Interstitial Ca occurs between the chains. Although brandtite, collinsite and fairfieldite are chemically quite similar, differences in their hydrogen-bonding arrangements result in significant structural differences. The three distinct structure-types are compared, with particular emphasis on the hydrogen-bonding arrangement in each structure. Several other structural arrangements are examined, based on different arrangements of hydrogen bonds involving the structural unit $[M^{2+}(\text{T}^{5+}\text{O}_4)_2(\text{H}_2\text{O})_2]$.

Keywords: brandtite, collinsite, fairfieldite, kröhnkite, crystal structure, hydrogen bonding.

SOMMAIRE

Nous avons affiné la structure cristalline de la brandtite $[\text{Ca}_2(\text{Mn,Mg})(\text{AsO}_4)_2(\text{H}_2\text{O})_2]$, monoclinique, a 5.877(1), b 12.957(2), c 5.675(1) Å, β 108.00(3)°, V 411.0 Å³, groupe d'espace $P2_1/c$, $Z = 2$], la collinsite $[\text{Ca}_2(\text{Mg,Fe})(\text{PO}_4)_2(\text{H}_2\text{O})_2]$, triclinique, a 5.729(1), b 6.778(1), c 5.444(1) Å, α 97.31(3), β 108.63(3), γ 107.25(3)°, V 189.8 Å³, groupe d'espace $P1$, $Z = 1$] et la fairfieldite $[\text{Ca}_2(\text{Mn,Mg})(\text{PO}_4)_2(\text{H}_2\text{O})_2]$, triclinique, a 5.795(1), b 6.576(1), c 5.495(1) Å, α 102.39(3), β 108.63(3), γ 90.29(3)°, V 194.0 Å³, groupe spatial $P1$, $Z = 1$] jusqu'à un résidu R de 2.6, 1.5 et 1.7%, respectivement, en utilisant 1200, 1089 et 1137 réflexions uniques $|F_o| > 5\sigma F$ mesurées avec un diffractomètre à quatre cercles automatisé muni d'un détecteur en série et avec un rayonnement MoK α . Ces structures sont fondées sur des chaînes infinies $[M(\text{TO}_4)_2(\text{H}_2\text{O})_2]$ parallèles à l'axe c , avec une période d'environ 5.55 Å. Les atomes interstitiels de Ca se situent entre les chaînes. Quoique la brandtite, la collinsite et la fairfieldite se ressemblent du point de vue chimique, les différences dans les agencements de leurs liaisons hydrogène sont la cause de différences structurales importantes. Les trois variantes distinctes du point de vue structural sont comparées, avec une attention particulière à l'agencement des liaisons hydrogène dans chaque structure. Plusieurs autres variantes structurales dépendent de différents agencements des liaisons hydrogène impliquant le module structural $[M^{2+}(\text{T}^{5+}\text{O}_4)_2(\text{H}_2\text{O})_2]$.

(Traduit par la Rédaction)

Mots-clés: brandtite, collinsite, fairfieldite, kröhnkite, structure cristalline, liaisons hydrogène.

INTRODUCTION

Minerals with the general formula $X_2M(\text{TO}_4)_2(\text{H}_2\text{O})_2$ are numerous and occur widely as minor or trace constituents in environments affected by hydrothermal alteration. They show a wide variety of octahedrally and tetrahedrally coordinated cations ($M = \text{Mg}, \text{Fe}^{2+}, \text{Mn}^{2+}, \text{Co}^{2+}, \text{Ni}, \text{Cu}^{2+}$; $T = \text{P}, \text{As}^{5+}, \text{S}^{6+}$), and yet the

interstitial X cation is almost always Ca, the one exception being kröhnkite, $\text{Na}_2\text{Cu}^{2+}(\text{SO}_4)_2(\text{H}_2\text{O})_2$, in which the interstitial cation is monovalent in order to maintain electroneutrality. Minerals of this general composition show three distinct structure-types (Table 1): the monoclinic *kröhnkite* group and the triclinic *talmesite* and *fairfieldite* groups. The crystal structure of kröhnkite was solved by Dahlman (1951) and refined

[§] E-mail address: frank_hawthorne@umanitoba.ca

by Hawthorne & Ferguson (1977). The crystal structure of collinsite was solved by Brotherton *et al.* (1974), and the structure of the isostructural talmessite was refined by Catti *et al.* (1977), who showed that the three distinct structure-types can be distinguished on the basis of cell parameters alone. The crystal structure of fairfieldite was solved by Fanfani *et al.* (1970). In addition, the structures of several other minerals of this type have since been refined (Table 1). Recently, there has been extensive work on the synthesis and structural characterization of synthetic analogues of these minerals, together with many other synthetic phases containing the $[M(\text{TO}_4)_2(\text{H}_2\text{O})_2]$ chain (Fleck *et al.* 2002a,b, 2003, Kolitsch & Fleck 2005) (Table 1). In particular, Fleck *et al.* (2002b) introduced a classification of these structures based on the space-group symmetry and geometrical relations between the chains and between the layers of chains and their interstitial cations.

There has been much work in the last twenty years on developing structural hierarchies or classifications of oxysalt minerals (Hawthorne 1984, 1985, 1986, 1990, 1992, 1994, 1997, Sabelli & Trosti-Ferroni 1985, Liebau 1985, Hawthorne *et al.* 1996, 2000, Hawthorne & Huminicki 2002, Huminicki & Hawthorne 2002, Burns 1999, Burns *et al.* 1996), focusing on the bond topology of the more strongly bonded cations (Hawthorne 1983). With much of this work now in place, it is important to focus on the bond topology of the interstitial species. It is these bonds that control the stability of minerals, as these weak bonds are more easily broken with changing conditions than the stronger bonds of the structural unit. As far as we are aware, these types of interactions have not been examined in terms of (1) the topology of the overall bond-arrangements, and (2) the geometry of the local interactions. Here, we examine this issue with

regard to the structures of the minerals of the brandtite, collinsite and fairfieldite groups.

EXPERIMENTAL

Provenance of the samples

The crystals used in this work come from the following sources: brandtite: Harstig mine, Harstigen, Sweden; collinsite: Rapid Creek, Yukon Territory, Canada; fairfieldite: Foote mine, North Carolina, U.S.A. Crystal sizes are given in Table 2. Each crystal was mounted with epoxy on a thin tapered glass fiber and mounted on a standard goniometer head.

TABLE 2. INFORMATION CONCERNING DATA COLLECTION AND REFINEMENT FOR BRANDTITE, COLLINSITE AND FAIRFIELDITE

	brandtite	collinsite	fairfieldite
<i>a</i> (Å)	5.877(1)	5.729(1)	5.795(1)
<i>b</i>	12.957(2)	6.778(1)	6.576(1)
<i>c</i>	5.675(1)	5.444(1)	5.496(1)
α (°)	90	97.31(3)	102.39(3)
β	108.00(3)	108.56(3)	108.63(3)
γ	90	107.25(3)	90.29(3)
<i>V</i> (Å ³)	411.06	185.6	193.25
Space group	<i>P</i> 2 ₁ / <i>c</i>	<i>P</i> 1	<i>P</i> 1
<i>Z</i>	2	1	1
Rad/Mon	MoKa/Gr	MoKa/Gr	MoKa/Gr
Total reflections	1365	2178	2274
Unique reflections	1200	1089	1137
<i>R</i> (merge) %	2.7	1.1	1.3
<i>R</i> %	2.6	1.5	1.7
<i>wR</i> ₂ (<i>F</i> ²)	6.5	4.1	4.7
GoF	0.939	0.932	0.943

$R = \frac{\sum(|F_o| - |F_c|)}{\sum|F_o|}$
 $wR = \frac{[\sum w(|F_o| - |F_c|)^2]}{[\sum w|F_o|^2]}^{1/2}$, $w = (1/\sigma^2(F) + 0.0005 F^2)^{-1}$

TABLE 1. MINERALS OF THE BRANDTITE, COLLINSITE AND FAIRFIELDITE GROUPS

Mineral	Formula (end-member)	<i>a</i> (Å)	<i>b</i> (Å)	<i>c</i> (Å)	α (°)	β (°)	γ (°)	Sp. gr.	Ref.
kröhnkite	Na ₂ Cu ²⁺ (SO ₄) ₂ (H ₂ O) ₂	5.807	12.656	5.517	90	108.32	90	<i>P</i> 2 ₁ / <i>c</i>	(1)
brandtite	Ca ₂ Mn ²⁺ (AsO ₄) ₂ (H ₂ O) ₂	5.877	12.957	5.675	90	108	90	<i>P</i> 2 ₁ / <i>c</i>	(2), (3)
roselite	Ca ₂ Co (AsO ₄) ₂ (H ₂ O) ₂	5.801	12.989	5.617	90	107.42	90	<i>P</i> 2 ₁ / <i>c</i>	(3)
wendwilsonite	Ca ₂ Mg (AsO ₄) ₂ (H ₂ O) ₂	5.806	12.912	5.623	90	107.4	90	<i>P</i> 2 ₁ / <i>c</i>	(4)
zincroselite	Ca ₂ Zn (AsO ₄) ₂ (H ₂ O) ₂	5.827	12.899	5.646	90	107.69	90	<i>P</i> 2 ₁ / <i>c</i>	(5)
cassidyite	Ca ₂ Ni (PO ₄) ₂ (H ₂ O) ₂	5.729	6.43	5.41	96.8	107.3	104.6	<i>P</i> 1	(6)
collinsite	Ca ₂ Mg (PO ₄) ₂ (H ₂ O) ₂	5.729	6.778	5.444	97.31	108.56	107.25	<i>P</i> 1	(2),(6)
talmessite	Ca ₂ Mg (AsO ₄) ₂ (H ₂ O) ₂	5.874	6.943	5.537	97.3	108.7	108.1	<i>P</i> 1	(7),(13)
gaiite	Ca ₂ Zn (AsO ₄) ₂ (H ₂ O) ₂	5.899	6.978	5.755	97.41	109.08	108.09	<i>P</i> 1	(8)
beta-roselite	Ca ₂ Co (AsO ₄) ₂ (H ₂ O) ₂	5.89	7.69	5.56	112.6	70.8	119.4	<i>P</i> 1	(9),(13)
parabrandtite	Ca ₂ Mn ²⁺ (AsO ₄) ₂ (H ₂ O) ₂	5.89	7.03	5.64	96.77	109.32	108.47	<i>P</i> 1	(10)
hillite	Ca ₂ Zn (PO ₄) ₂ (H ₂ O) ₂	5.736	6.767	5.462	97.41	108.59	107.19	<i>P</i> 1	(11)
fairfieldite	Ca ₂ Mn ²⁺ (PO ₄) ₂ (H ₂ O) ₂	5.795	6.576	5.496	102.39	108.63	90.29	<i>P</i> 1	(2),(12)
messelite	Ca ₂ Fe ²⁺ (PO ₄) ₂ (H ₂ O) ₂	5.95	6.52	5.45	102.3	107.5	90.8	<i>P</i> 1	(9)

References: (1) Hawthorne & Ferguson (1975), (2) this study, (3) Hawthorne & Ferguson (1977), Hejny *et al.* (1997), (4) Dunn *et al.* (1987a), (5) Keller *et al.* (1986, 2002, 2004), (6) Brotherton *et al.* (1974), (7) Catti *et al.* (1977), (8) Keller *et al.* (2004), Sturman & Dunn (1980), (9) Frondel (1955), (10) Dunn *et al.* (1987b), (11) Yakubovich *et al.* (2003), (12) Fanfani *et al.* (1970), (13) Joswig *et al.* (2004).

Collection of X-ray intensity data

The unit-cell dimensions were determined using a Bruker P4 automated four-circle single-crystal X-ray diffractometer equipped with a serial detector and a MoK α X-ray source. The SHELXTL PC software was used for data reduction and least-squares refinement. For brandtite, 25 reflections between 10 and 30° 2 θ were centered, and a constrained monoclinic cell was determined from the setting angles and refined using least squares. For collinsite and fairfieldite, 25 reflections between 10 and 30° 2 θ were centered and a triclinic cell was determined and refined in the same manner. Miscellaneous information on collection and refinement of the data is listed in Table 2. We measured single-crystal intensity data from 4 to 60° 2 θ with a scan range of 1.2° and scan speeds from 2.0 to 29°/min. Psi-scan data were measured on 20 reflections out to 60° 2 θ at 5° increments for absorption corrections, and we modeled each crystal as a triaxial ellipsoid. Intensities were subsequently corrected for Lorentz, polarization and background effects.

Electron-microprobe analysis

The crystals used for X-ray data collection were mounted in epoxy on 2.5-cm-diameter Perspex discs, ground, polished, carbon-coated and analyzed with a Cameca SX-100 electron microprobe operating under the following conditions in wavelength-dispersion mode: excitation voltage: 15 kV, specimen current: 20 nA, beam size: 5 μ m, peak count-time: 20 s, background count-time: 10 s. We used the following standards and crystals for K α X-ray lines: Mg: forsterite; Fe: fayalite; Mn: spessartine; Co: CoNb₂O₆; Ni: NiSi; Zn: gahnite; P: apatite; As: cobaltite; S: chalcopyrite,

Ca: diopside. Five points on each crystal were analyzed. Back-scattered-electron images of each crystal show no sign of compositional zoning. The chemical formulae were calculated on the basis of ten anions with (OH) = 4 *apfu* (atoms per formula unit). Chemical compositions and unit formulae are given in Table 3.

CRYSTAL-STRUCTURE REFINEMENT

All calculations were done with the SHELTXL PC Plus software package. Crystal-structure refinements of brandtite, collinsite and fairfieldite were initiated with the atom coordinates of roselite (Hawthorne & Ferguson 1977), collinsite (Brotherton *et al.* 1974) and fairfieldite (Fanfani *et al.* 1970), respectively. We located the H positions using difference-Fourier maps, and imposed a restraint on the refinements such that the O–H distance should be close to 0.98 Å by adding extra weighted observational equations to the least-squares matrix. This procedure results in more realistic geometry for the hydrogen bonds. Refinement converged to *R*-indices of 2.6, 1.5 and 1.7%, respectively. Final positional and displacement parameters are given in Table 4, selected interatomic distances are listed in Table 5, refined site-scattering values (Hawthorne *et al.* 1995) are given in Table 6, details of the hydrogen bonds are listed in Table 7, and bond valences are given in Table 8. Observed and calculated structure-factors may be obtained from The Depository of Unpublished Data, CISTI, National Research Council, Ottawa, Ontario K1A 0S2, Canada.

DESCRIPTION OF THE STRUCTURES

The *T*-site atoms are normally As⁵⁺ and P, and are surrounded by a regular tetrahedral arrangement of O atoms. The *M*-site atoms are normally divalent and are surrounded by an octahedral arrangement of four O atoms and two (H₂O) groups. The *X*-site atoms are commonly Ca and are surrounded by an irregular [8]-coordinated polyhedral arrangement of seven O atoms and one (H₂O) group. All three structure-types are based on infinite [*M*(TO₄)₂(H₂O)₂] chains that extend in the *c* direction with a repeat distance of ~5.55 Å. These chains are linked into continuous structures by interstitial Ca atoms and by hydrogen bonds involving the (H₂O) groups (Fig. 1), and it is these linkages on which we will focus here. For direct comparison, the atoms in each structure have been relabeled such that they are topologically equivalent (Fig. 2).

The three structures seem very similar (Fig. 1). However, significant differences are apparent in the linkage of the (Ca ϕ ₈) polyhedra. In all three structures, the (Ca ϕ ₈) polyhedra form edge-sharing dimers; however, the different linkages between these dimers give rise to three distinctly different sheets of polyhedra (Fig. 3). In brandtite (Fig. 3a), dimers share edges with other dimers along the *c* direction to form zig-zag

TABLE 3. CHEMICAL COMPOSITION (wt.%) AND UNIT FORMULAE* (*apfu*) FOR BRANDTITE, COLLINSITE AND FAIRFIELDITE

	Brandtite	Collinsite	Fairfieldite
P ₂ O ₅	–	42.13	39.34
As ₂ O ₅	49.58	–	–
CaO	23.15	33.54	30.60
MgO	0.86	11.07	0.06
MnO	13.36	0.15	14.26
FeO	0.08	1.31	4.49
PbO	2.48	–	–
H ₂ O**	7.68	10.71	9.89
Total***	97.19	98.91	98.64
X: Ca	1.94	2	2
Pb ²⁺	0.05	–	–
Y: Mg	0.10	0.92	0.01
Mn	0.88	0.01	0.73
Fe	0.01	0.06	0.23
ΣY	0.99	0.99	0.97
T: P	–	2	2
As	2	–	–

* Formulae normalized to 10 anions. ** H₂O calculated by stoichiometry.
*** No other elements were found to be above the detection limits.

TABLE 4. ATOM COORDINATES AND ANISOTROPIC-DISPLACEMENT PARAMETERS

Site	x	y	z	U_{eq}	U_{11}	U_{22}	U_{33}	U_{23}	U_{13}	U_{12}
<i>brandtite</i>										
X=Ca	0.56763(11)	0.11965(5)	0.24347(11)	0.0095(2)	0.0095(3)	0.0091(3)	0.0101(3)	-0.0012(2)	0.0034(2)	-0.0011(2)
M=Mn	0	0	0	0.0094(2)	0.0096(4)	0.0089(4)	0.0093(4)	-0.0041(3)	0.0023(3)	-0.0009(3)
T=As	0.22243(5)	0.12174(2)	0.57383(6)	0.00639(11)	0.00747(16)	0.00533(16)	0.00581(16)	0.00021(12)	0.00123(11)	0.00010(11)
O(1)	0.2445(4)	0.03619(19)	0.3558(5)	0.0119(5)	0.0128(11)	0.0120(12)	0.0111(11)	-0.0061(9)	0.0040(9)	-0.0019(9)
O(2)	0.2883(4)	0.05599(19)	0.8451(4)	0.0094(4)	0.0096(10)	0.0090(11)	0.0077(10)	0.0034(9)	0.0000(8)	-0.0000(8)
O(3)	0.9499(4)	0.17265(19)	0.5022(5)	0.0110(5)	0.0084(10)	0.0092(11)	0.0139(12)	0.0005(9)	0.0013(9)	0.0034(8)
O(4)	0.4404(4)	0.20712(19)	0.5795(4)	0.0099(4)	0.0098(10)	0.0084(11)	0.0112(11)	-0.0010(9)	0.0028(8)	-0.0038(8)
OW	0.8087(4)	0.14270(19)	0.9719(4)	0.0099(5)	0.0132(11)	0.0089(11)	0.0067(10)	0.0005(9)	0.0018(8)	-0.0020(8)
H(1)	0.685(6)	0.150(4)	0.811(4)	0.037(15)						
H(2)	0.907(6)	0.205(2)	0.987(9)	0.028(13)						
<i>collinsite</i>										
X=Ca	0.30332(5)	0.75897(4)	0.65422(5)	0.00910(8)	0.00765(12)	0.01038(12)	0.00879(12)	0.00116(8)	0.00351(9)	0.00259(9)
M=Mg	0	0	0	0.0076(2)	0.0058(3)	0.0098(3)	0.0064(3)	0.00095(18)	0.00196(19)	0.00258(19)
T=P	0.33308(6)	0.24382(5)	0.66329(6)	0.00577(8)	0.00513(14)	0.00637(14)	0.00578(14)	0.00174(10)	0.00175(10)	0.00225(10)
O(1)	0.25585(18)	0.07243(15)	0.40377(18)	0.00989(18)	0.0098(4)	0.0102(4)	0.0078(4)	-0.0007(3)	0.0019(3)	0.0037(3)
O(2)	0.33308(18)	0.12722(15)	0.89146(18)	0.00899(17)	0.0088(4)	0.0109(4)	0.0089(4)	0.0055(3)	0.0037(3)	0.0040(3)
O(3)	0.15488(18)	0.37340(14)	0.63328(18)	0.00907(17)	0.0091(4)	0.0098(4)	0.0104(4)	0.0036(3)	0.0036(3)	0.0058(3)
O(4)	0.61936(17)	0.38661(14)	0.72049(18)	0.00948(17)	0.0064(4)	0.0100(4)	0.0100(4)	0.0024(3)	0.0025(3)	0.0007(3)
OW	0.94947(18)	0.27786(14)	0.06803(18)	0.00884(17)	0.0084(4)	0.0084(4)	0.0088(4)	0.0024(3)	0.0023(3)	0.0025(3)
H(1)	0.838(4)	0.316(4)	-0.077(4)	0.039(7)						
H(2)	1.117(3)	0.392(3)	0.144(5)	0.050(8)						
<i>fairfieldite</i>										
X=Ca	0.6010(1)	0.2337(1)	0.3329(1)	0.0091(1)	0.0093(2)	0.0090(2)	0.0086(2)	0.0012(1)	0.0030(1)	0.0002(1)
M=Mn	0	0	0	0.0095(1)	0.0095(2)	0.0105(2)	0.0071(2)	-0.0001(1)	0.0020(1)	0.0005(1)
T=P	0.2452(1)	0.2324(1)	0.6475(1)	0.0070(1)	0.0083(2)	0.0065(2)	0.0059(2)	0.0018(1)	0.0017(1)	0.0004(1)
O(1)	0.2451(2)	0.0693(2)	0.3961(2)	0.0111(2)	0.0129(5)	0.0108(4)	0.0078(4)	-0.0007(3)	0.0030(4)	-0.0004(4)
O(2)	0.3050(2)	0.1179(2)	0.8781(2)	0.0101(2)	0.0117(4)	0.0105(4)	0.0086(4)	0.0048(3)	0.0024(3)	0.0009(3)
O(3)	0.0021(2)	0.3271(2)	0.6145(1)	0.0106(2)	0.0097(4)	0.0103(4)	0.0114(4)	0.0032(3)	0.0024(3)	0.0020(3)
O(4)	0.4545(2)	0.3994(2)	0.6957(2)	0.0100(2)	0.0106(4)	0.0081(4)	0.0110(4)	0.0021(3)	0.0034(3)	-0.0007(3)
OW	-0.1529(2)	0.2999(2)	0.0674(2)	0.0119(2)	0.0154(5)	0.0102(4)	0.0090(4)	0.0015(4)	0.0029(4)	0.0011(4)
H(1)	-0.277(4)	0.346(5)	-0.071(5)	0.052(9)						
H(2)	-0.072(5)	0.432(3)	0.181(5)	0.054(9)						

TABLE 5. SELECTED INTERATOMIC DISTANCES (Å) FOR BRANDTITE, COLLINSITE AND FAIRFIELDITE

	brandtite		collinsite		fairfieldite
Ca-O(1)	2.435(3)	Ca-O(1)h	2.583(1)	Ca-O(1)	2.478(1)
Ca-O(1)a	2.986(3)	Ca-O(1)l	2.700(1)	Ca-O(1)a	2.725(1)
Ca-O(2)c	2.489(3)	Ca-O(2)j	2.517(2)	Ca-O(2)c	2.490(1)
Ca-O(2)e	2.533(3)	Ca-O(2)l	2.591(1)	Ca-O(2)a	2.501(1)
Ca-O(3)	2.374(3)	Ca-O(3)	2.472(1)	Ca-O(3)n	2.336(1)
Ca-O(4)	2.522(3)	Ca-O(3)k	2.403(1)	Ca-O(4)	2.458(1)
Ca-O(4)b	2.453(3)	Ca-O(4)h	2.378(1)	Ca-O(4)h	2.467(1)
Ca-Ow	2.413(3)	Ca-Owh	2.392(1)	Ca-Owh	2.439(1)
<Ca-O>	2.526	<Ca-O>	2.505	<Ca-O>	2.487
M-O(1) x2	2.138(2)	M-O(1)d x2	2.114(1)	M-O(1)d x2	2.136(1)
M-O(2)c,e x2	2.256(2)	M-O(2)c,e x2	2.146(1)	M-O(2)c,e x2	2.268(1)
M-Owf,a x2	2.144(2)	M-Owl,m x2	1.996(1)	M-Owd x2	2.174(1)
<M-O>	2.179	<M-O>	2.085	<M-O>	2.193
T-O(1)	1.896(2)	T-O(1)	1.556(1)	T-O(1)	1.557(1)
T-O(2)	1.896(2)	T-O(2)	1.555(1)	T-O(2)	1.557(1)
T-O(3)g	1.662(2)	T-O(3)	1.517(1)	T-O(3)	1.516(1)
T-O(4)	1.685(2)	T-O(4)	1.543(1)	T-O(4)	1.551(1)
<T-O>	1.685	<T-O>	1.543	<T-O>	1.545

Symmetry operators: a = -x + 1, -y, -z + 1; b = x, -y + 1/2, z - 1/2; c = x, y, z - 1; d = -x, -y, -z; e = x - 1, y, z - 1; f = x - 1, y, z + 1; g = x - 1, -y + 1/2, z + 1/2; h = -x + 1, -y + 1, -z + 1; i = x, y + 1, z; j = -x + 1, -y + 1, -z + 2; k = -x, -y + 1, -z + 1; l = x - 1, y, z; m = -x + 1, -y, -z; n = x + 1, y, z.

TABLE 6. REFINED AND ASSIGNED SITE-SCATTERING VALUES ($epfu^*$) FOR SELECTED SITES

	X site refined**	X site assigned***	Y site refined**	Y site assigned
Brandtite	40.6(1)	42.9	23.56(1)	23.5
Collinsite	40	40.2	13.12(5)	12.9
Fairfieldite	40	40.6	25.08(5)	24.7

* electrons per formula unit.

** all X sites were refined as Ca; the Y site of brandtite and fairfieldite was refined as Mn, and the Y site of collinsite was refined as Mg.

*** assigned from chemical formula.

chains that link in the *b* direction by sharing polyhedron corners. The resultant sheet is parallel to (100), and each polyhedron shares two edges and two vertices with the four adjacent polyhedra. In collinsite (Fig. 3b), dimers share edges with other dimers along the [011] and [01 $\bar{1}$] directions to form a sheet in which all linkages involve sharing of polyhedron edges. This sheet is parallel to (110), and each polyhedron shares three edges with the

three adjacent polyhedra. In fairfieldite (Fig. 3c), dimers share edges with other dimers along the *c* direction to form zig-zag chains, and the polyhedra of these chains share edges with the polyhedra of chains adjacent in the *b* direction, again forming a sheet in which all linkages occur through polyhedron edges. The resultant sheet is parallel to (100), and each polyhedron shares three edges with the three adjacent polyhedra.

INTERSTITIAL LINKAGE

The interstitial interactions are particularly interesting in these groups of minerals, as the structural units are topologically identical in all three groups. There are three distinct factors involved in the interstitial linkage of the chains: (1) the attitude and offset of the adjacent chains, (2) the coordination of Ca by anions of adjacent chains, and (3) the arrangement of hydrogen bonds. As noted above, the differences in these three aspects of these structures are of considerable interest, not least because of the topological identity of the structural units in all three groups.

Attitude of adjacent chains

In brandtite, the upper faces of the octahedra of adjacent chains [when the structures are viewed perpendicular to (011)] point in alternate directions (see red arrows, Fig. 1a), whereas in collinsite and fairfieldite, the corresponding faces of octahedra of adjacent chains point in the same direction (Figs. 1b, c). In brandtite, the chains adjacent in the *b* direction are tilted in opposite directions, imparting a wave-like modulation to the sheet of (Ca ϕ_8) polyhedra (Fig. 1d). In collinsite, the chains adjacent in the *b* direction are tilted in the same direction; when combined with the relative displacement of adjacent chains (Fig. 1e), this results in the sheet of (Ca ϕ_8) polyhedra being parallel to (10 $\bar{1}$). In fairfieldite, the chains adjacent in the *b* direction are

tilted in the same direction which, when combined with the absence of a relative displacement of adjacent chains (Fig. 1f), results in a modulated sheet of (Ca ϕ_8) polyhedra parallel to (100).

Interchain linkage by interstitial Ca

The linkage of adjacent chains in all three structure types is shown in Figure 4, where adjacent chains are labeled (i) through (iv). Inspection shows that in brandtite (Fig. 4a), Ca (highlighted by the circle) links chains (i), (ii) and (iii), whereas in collinsite (Fig. 4b) and fairfieldite (Fig. 4c), Ca links chains (ii), (iii) and (iv). This difference in the linkage of adjacent chains is a result of the difference in attitude of the chains in the *b* direction in these structures (Fig. 1). In brandtite, the octahedron faces of adjacent chains point in opposing directions (Fig. 1a). This has the effect of tilting the tetrahedra of adjacent chains in opposing directions relative to the octahedra to which they are linked (Fig. 4a), and the tetrahedra of chain (i) are within bonding range of the Ca under consideration. In

TABLE 8. BOND-VALENCE (νu)* TABLES

	Ca	M^{2+}	T^{5+}	H(1)	H(2)	Σ
<i>brandtite</i>						
O(1)	0.28 0.07	0.39 ²² 1	1.21			1.95
O(2)	0.24 0.21	0.28 ²² 1	1.21			1.94
O(3)	0.33		1.33		0.30	1.96
O(4)	0.22 0.27		1.25	0.30		2.04
OW	0.30	0.38 ²² 1		0.70	0.70	2.08
Sum	1.92	2.10	5.00	1.00	1.00	
<i>collinsite</i>						
O(1)	0.19 0.14	0.32 ²² 1	1.18			1.83
O(2)	0.23 0.19	0.29 ²² 1	1.18			1.89
O(3)	0.26 0.31		1.31			1.88
O(4)	0.33		1.22	0.30	0.30	2.15
OW	0.32	0.44 ²² 1		0.70	0.70	2.16
Sum	1.97	2.10	4.89	1.00	1.00	
<i>fairfieldite</i>						
O(1)	0.25 0.13	0.39 ²² 1	1.18			1.95
O(2)	0.24 0.24	0.28 ²² 1	1.18			1.94
O(3)	0.37		1.31		0.30	1.98
O(4)	0.27 0.26		1.19	0.30		2.02
OW	0.28	0.35 ²² 1		0.70	0.70	2.03
Sum	2.04	2.04	4.86	1.00	1.00	

TABLE 7. SELECTED DONOR (D) OXYGEN – HYDROGEN – ACCEPTOR (A) OXYGEN INTERATOMIC DISTANCES (Å) AND ANGLES (°) FOR BRANDTITE, COLLINSITE AND FAIRFIELDITE

	brandtite	collinsite	fairfieldite
H(1)–OW	0.98(1)	0.96(1)	0.98(1)
H(2)–OW	0.98(1)	0.98(1)	0.98(1)
H(1)...A(1)*	1.78(2)	1.604(6)	1.753(7)
H(2)...A(2)*	1.61(2)	1.633(5)	1.685(8)
OW–A(1)	2.712(3)	2.5699(16)	2.720(2)
OW–A(2)	2.521(4)	2.6060(19)	2.646(2)
OW–H(1)–A(1)	157(5)	168(2)	168(3)
OW–H(2)–A(2)	153(4)	171(3)	166(3)
H(1)–OW–H(2)	105(4)	107(2)	101(3)

* brandtite: A(1) = O(4); A(2) = O(3); collinsite: A(1) = O(4); A(2) = O(4); fairfieldite: A(1) = O(4); A(2) = O(3).

* calculated with the parameters of Brown & Altermatt (1985).

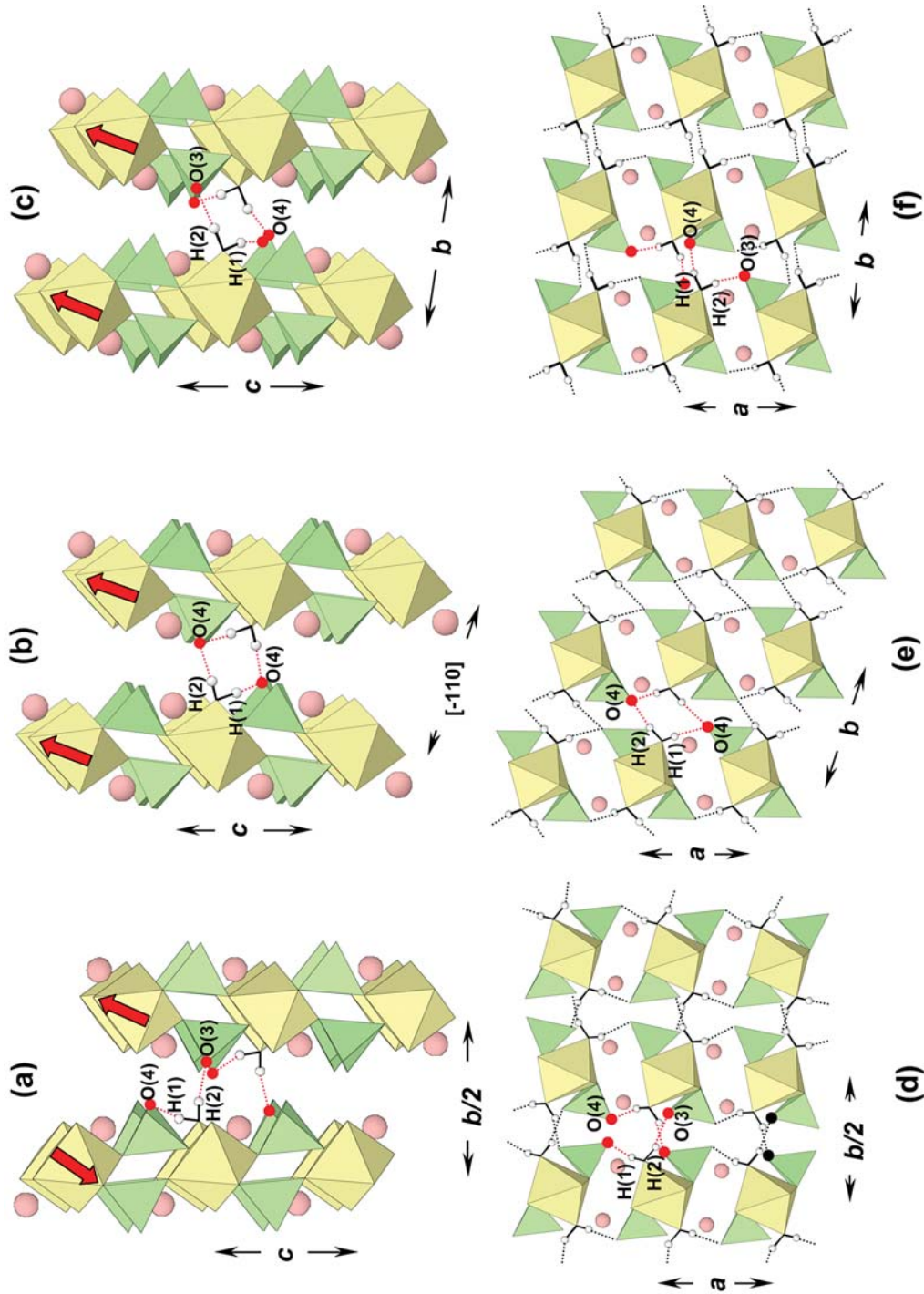


FIG. 1. The crystal structures of (a), (d) brandite, (b), (e) collinsite, and (c), (f) fairfieldite projected onto (100). *M* octahedra are lemon yellow, *T* tetrahedra are pale green, Ca is tan, and H are small white circles. Hydroxyl bonds are shown as solid lines, hydrogen bonds are shown as red or black dotted lines, and acceptor anions for (red) hydrogen bonds are shown as red circles. The red arrows show the relative attitude of the octahedra in adjacent chains.

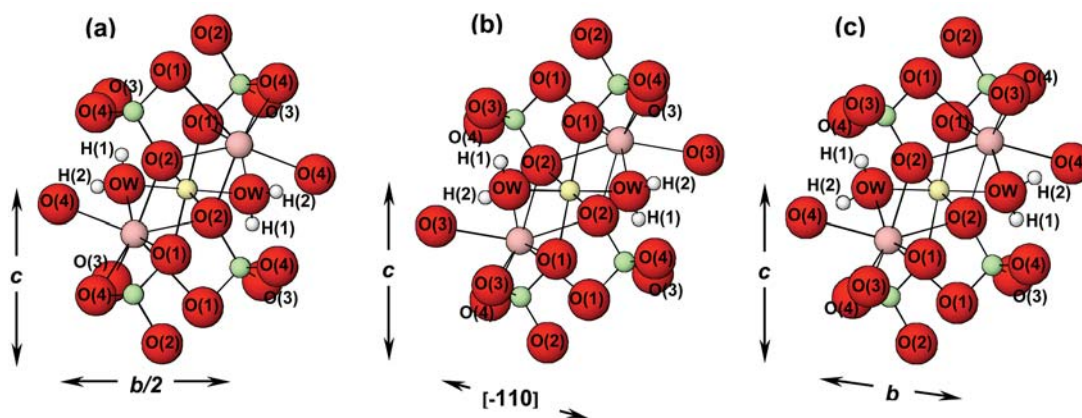


FIG. 2. The new atom-labeling schemes in (a) brandtite, (b) collinsite, and (c) fairfieldite. Legend as in Figure 1, oxygen atoms are shown as large red circles.

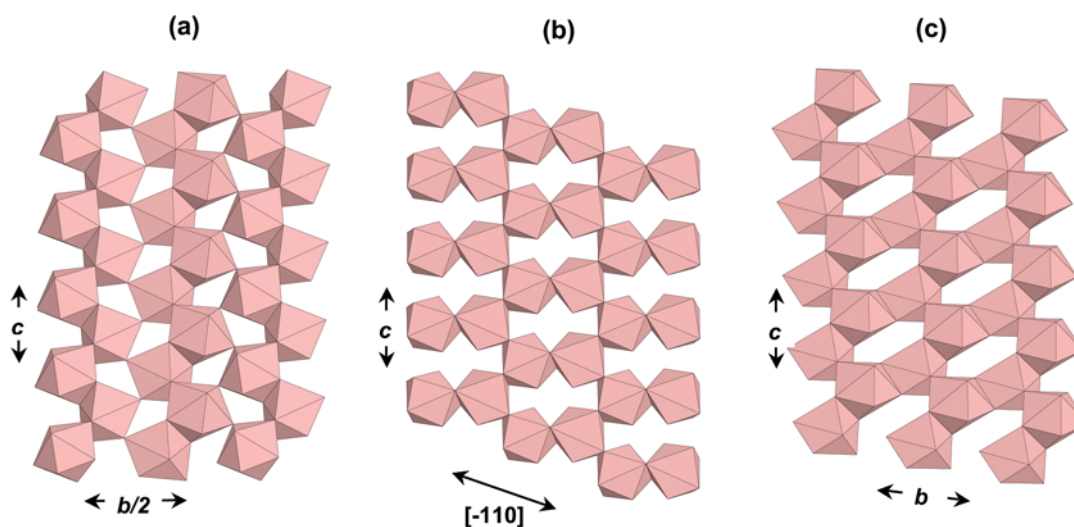


FIG. 3. The layers formed by Ca polyhedra in (a) brandtite, (b) collinsite, and (c) fairfieldite; the layers are parallel to (010), (110) and (010), respectively.

collinsite and fairfieldite, the chains point in the same directions (Figs. 1e, 1f). This has the effect of tilting the tetrahedra of adjacent chains in the same direction relative to the octahedra to which they are linked (Figs. 4b, 4c), and the tetrahedra of chain (iv) are within bonding range of the Ca under consideration.

So what is the difference in the interchain linkage by Ca in collinsite and fairfieldite? Close inspection of Figures 4b and 4c shows that the linkage between Ca and chain (iii) is the same in both structures [Ca bonds to O(1)a, O(2)a, O(3)a and OW, see extracted view of

the $(Ca\phi_8)$ polyhedra (ϕ : unspecified anion) for each structure, Fig. 4]. Furthermore, the linkage between Ca and chain (ii) is the same in both structures: Ca bonds to O(1)b, O(2)b and O(4)b (Figs. 4b, 4c). So seven of the eight Ca- ϕ bonds are the same in collinsite and fairfieldite. The difference between the interchain linkage by Ca in these two structures involves their linkage to chain (iv). In collinsite, Ca links to O(3)c in chain (iv) (Fig. 4b), whereas in fairfieldite, Ca links to O(4)c in chain (iv) (Fig. 4c). The reason for this difference is also apparent in Figure 4. In both structures, the inter-

stitial Ca links to the same tetrahedron (Figs. 4b, c). However, in collinsite, chain (iii) is further along the *a* direction than it is in fairfieldite; this has the effect of switching the linkage from one end of the tetrahedron in fairfieldite to the other end of the tetrahedron in collinsite.

Interstitial hydrogen-bond arrangements

The stereochemical details of the hydrogen-bonding network in each structure type are given in Table 7. Inspection of Figures 1a, b and c shows that in all three structure-types, the $[M(TO_4)_2(H_2O)_2]$ chains are repeated by the *a* translation to form layers of discon-

nected chains parallel to (100). Inspection of these layers (Figs. 5a, b, c) shows that the arrangement of hydrogen bonds is the same within these layers in each structure-type: the H(1) atom hydrogen-bonds to the O(4) anion, and the arrangement is the same in each case. This observation indicates that the structural differences among the minerals of these three groups must arise from differences in hydrogen-bond arrangements *between* these layers.

The hydrogen bonds involved in linkage between layers can be seen in Figures 1d, e, f. Inspection of Figures 1e, f indicate that (1) in the layers adjacent in the [010] direction, the constituent octahedra "point" in the same direction, and (2) the interlayer hydrogen

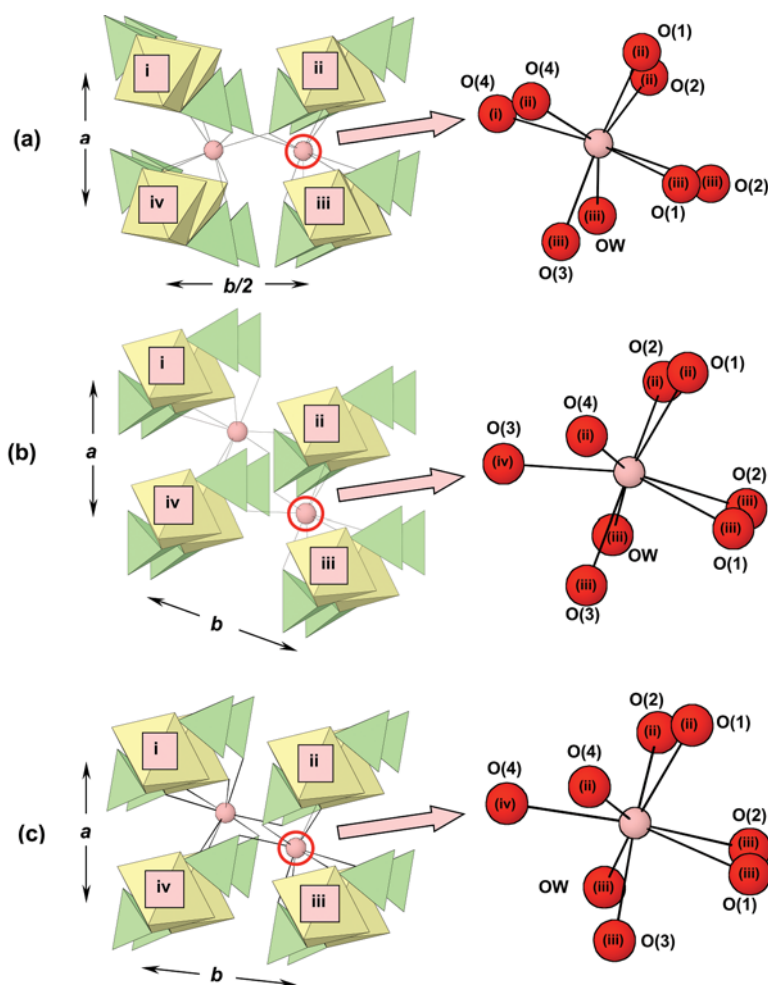


FIG. 4. The crystal structures of (a) brandtite, (b) collinsite, and (c) fairfieldite, projected onto (001), showing the coordination of Ca by anions of different chains. Legend as in Figures 1 and 2. The chains are labeled (i) to (iv), and the anions are labeled accordingly.

bond links to different anions of the tetrahedron in the adjacent layer (Figs. 1e, f). In the projection of Figures 1e, f, there are no other hydrogen-bond arrangements possible. Inspection of Figure 1d indicates that (1) the layers adjacent in the [010] direction “point” in opposite directions, and (2) the interlayer hydrogen bond links to the upper anion of the tetrahedron in the adjacent layer.

OTHER POSSIBLE HYDROGEN-BONDING ARRANGEMENTS

Inspection of Figure 1 and Table 7 indicates that the acceptor anions for the hydrogen-bond arrangements are invariably the O(3) or O(4) anions of the (TO_4) tetrahedron. In terms of the atoms that are involved in these arrangements, the following connections are topologically (but not necessarily stereochemically) possible: (1) H(1)...O(3), H(2)...O(3); (2) H(1)...O(4), H(2)...O(4); (3) H(1)...O(3), H(2)...O(4); (4) H(1)...O(4), H(2)...O(3). Arrangement (2) occurs in collinsite,

and arrangement (4) occurs in brandtite and fairfieldite. In order for the other two arrangements to occur with a reasonable stereochemistry, H(1) and H(2) would have to exchange positions, and thus the arrangements would be the same as those of (2) and (4), only the atom labeling would be different. Hence the arrangements observed are the only ones possible with respect to the current labeling of the atoms.

A possible new structural arrangement with $P2_1/n$ symmetry

The description of the intersheet arrangements of hydrogen bonds given above suggests the possibility of another arrangement. In Figures 1e, f, we see that the intersheet hydrogen-bond links to the bottom and top, respectively, of the tetrahedron in the adjacent layer, whereas in Figure 1d, the interlayer hydrogen-bond links to the bottom of the tetrahedron in the adjacent layer. This arrangement suggests the possibility of inter-layer hydrogen-bonds linking to the top anion of the

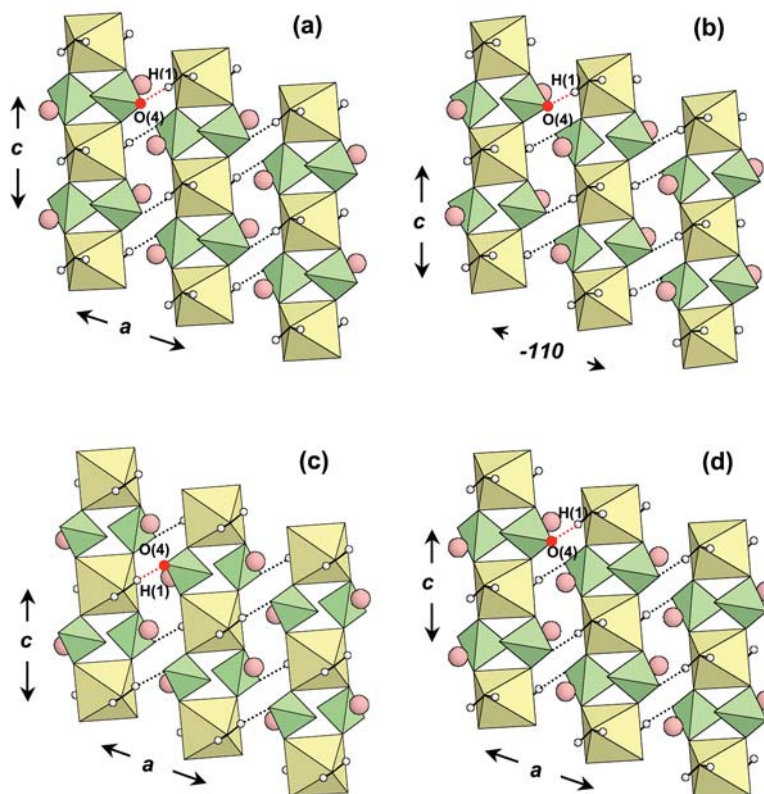


FIG. 5. The crystal structures of (a) brandtite, (b) collinsite, (c) fairfieldite, and (d) a hypothetical $P2_1/n$ structure of the same stoichiometry, projected onto (010), showing the layers of $[M(TO_4)_2(H_2O)_2]$ chains and the intralayer hydrogen-bonds. Legend as in Figure 1.

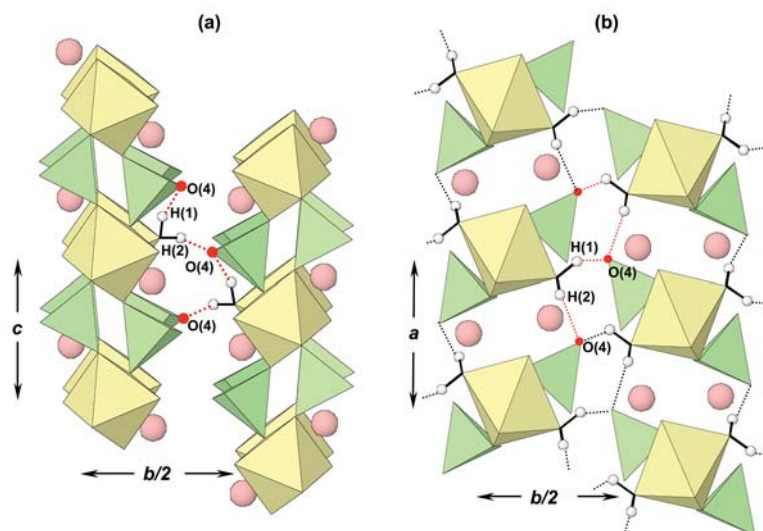


FIG. 6. The crystal structure of a hypothetical $P2_1/n$ structure of $\text{Ca}_2M^{2+}(\text{TO}_4)_2(\text{H}_2\text{O})_2$ stoichiometry (a) projected onto (100), and (b) projected onto (001), showing the network of inter- and intralayer hydrogen-bonds. Legend as in Figure 1.

tetrahedron in an adjacent layer in which the octahedron points in the opposite direction. In terms of Figure 1d, such a linkage would require a shift of adjacent layers by $\sim a/2$. This would have the result of producing a monoclinic structure with an n glide (instead of a c glide as in brandtite). This structure arrangement is shown in Figure 6, using the cell dimensions for brandtite, and the atom positions and interatomic distances are given in Tables 4 and 5. The arrangement of hydrogen bonds *within* the layers of chains is the same as in the other structure-types (Fig. 5d), but the hydrogen bonds *between* layers link to the top anion of the tetrahedron in the adjacent layer [*i.e.*, the O(4) anion (Fig. 6b) rather than the O(3) anion as in brandtite (Fig. 1d)]. Of course, the layer of X-cation polyhedra in the $P2_1/n$ structure will also be different (Fig. 7). Although this layer superficially resembles the analogous sheet in brandtite (Fig. 3a), careful inspection shows that the chains of edge-sharing polyhedra extending in the c direction cross-link to different vertices of chains adjacent in the [010] direction (Fig. 7).

Inspection of the bond-valence tables for these three structure-types (Table 8) shows that the valence-sum rule (Brown 1981, Hawthorne 1992, 1994, 1997) is obeyed reasonably well in all structures. We may evaluate the degree of agreement for each structure by calculating the RMS (root mean-square) deviation for the anions of each structure. The resulting values are 0.056, 0.144 and 0.039 vu for brandtite, collinsite and fairfieldite, respectively. Our experience with oxysalt structures indicates that RMS deviations are usually

$<0.15 vu$, in accord with the results obtained here. For the $P2_1/n$ arrangement derived above, the RMS deviation is $\sim 0.23 vu$, suggesting that this arrangement will not be stable owing to excessive deviation from the valence-sum rule.

How can the collinsite structure accommodate two hydrogen-bonds to the O(4) anion and no hydrogen bonds to the O(3) anion, whereas the $P2_1/n$ structure cannot? This issue involves the coordination of the interstitial Ca atom in each structure. In collinsite, Ca has two bonds to O(3) and one bond to O(4), resulting in O(3) and O(4) coordination numbers of [3] and [4], respectively (Table 8). In brandtite, Ca has one bond to O(3) and two bonds to O(4), resulting in O(3) and O(4) coordination numbers of [3] and [4], respectively (Table 8). In the $P2_1/n$ arrangement, Ca bonds to one O(3) and two O(4) atoms, resulting in coordination numbers of [2] and [5] for O(3) and O(4), respectively. It is this difference in bond topology that results in the major deviations from the valence-sum rule for the $P2_1/n$ arrangement.

Other possible arrangements

Another possibility of different arrangements arises if we consider the same labeled arrangements, but consider atoms *in different layers*. This issue is illustrated in Figure 8 for triclinic structures of symmetry $P\bar{1}$. Starting from the fairfieldite structure, the γ angle is decreased relative to that in fairfieldite, which has the effect of shifting the chains parallel to [100] relative

to each other (indicated by the arrows in Fig. 8) and allowing the H(1) atom to hydrogen-bond to the O(4) anion in the adjacent layer rather than in the same layer (as it does in fairfieldite). As there are no changes in coordination number of any of the anions in Figure 8 (relative to Fig. 1f), there are no obvious deviations from the valence-sum rule, and there is no convincing structural reason apparent to us why the arrangement of Figure 8 could not occur. Similar angular shear on the collinsite structure does not modify the hydrogen-bond arrangement.

COMPOSITIONAL ASPECTS OF THE $X_2[M(TO_4)_2(H_2O)_2]$ STRUCTURES

Inspection of Table 1 shows there are both similarities and differences with regard to the chemical compositions of the minerals in these three groups:

(1) the brandtite-group minerals are all arsenates (with the exception of kröhnkite, which is the only sulfate mineral in any of these groups).

(2) The fairfieldite-group minerals are all phosphates.

(3) The collinsite-group minerals are both phosphates and arsenates.

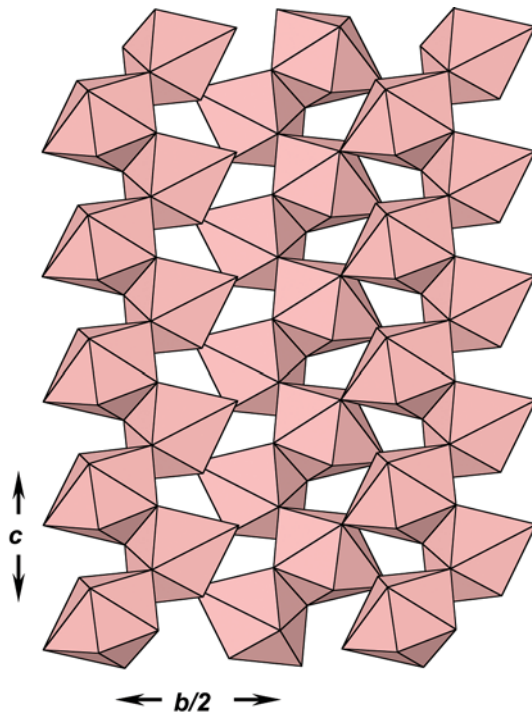


FIG. 7. The layer of Ca polyhedra in the hypothetical $P2_1/n$ structure. Legend as in Figure 3.

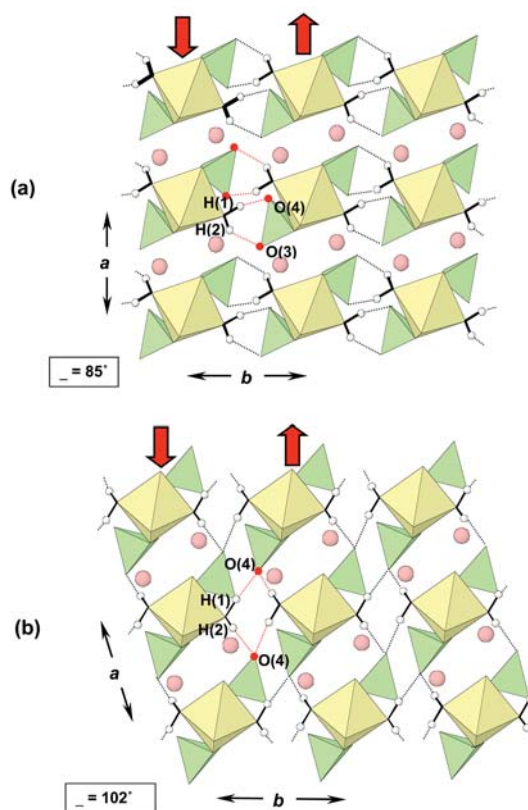


FIG. 8. A different hydrogen-bond arrangement produced from the fairfieldite arrangement by changing the γ angle. Legend as in Figure 1.

(4) There are no vanadate minerals in any of these groups.

(5) There is considerable polymorphism among the arsenate minerals of these groups: the compositions $Ca_2Mg(AsO_4)_2(H_2O)_2$ (wendwilsonite and talmessite), $Ca_2Co(AsO_4)_2(H_2O)_2$ (roselite and beta-roselite) and $Ca_2Mn^{2+}(AsO_4)_2(H_2O)_2$ (brandtite and parabrantite) occur as both structure-types.

(6) All minerals (except kröhnkite) have Ca as the dominant X-cation.

The X-cation may be monovalent (Na in kröhnkite) or divalent (Ca in all the other minerals of these three groups). Fleck & Kolitsch (2003), Kolitsch & Fleck (2005) and Fleck *et al.* (2002b) have reviewed both minerals and synthetic compounds based on the $[M(TO_4)_2(H_2O)_2]$ chains and have shown that there are a wide variety of synthetic compounds with $X = Na, K, Rb, Cs, NH_4$. Curiously, there are no synthetic compounds with $X = Ca$, and no minerals (apart from kröhnkite) with monovalent X-cations. Hawthorne

(1985) used the valence-matching principle (Brown 1981) to account for the fact that no minerals of these structure types occur with other divalent cations (*e.g.*, Ba, Sr, Pb^{2+}) dominant at the X site. Liferovich *et al.* (2001) reported Sr up to 0.37 *apfu* in collinsite from the Kovdor carbonatite. One can account for the incorporation of a less-than-ideal cation (in terms of the valence-matching principle) into the structure by locally associating the cation with structural strain. However, where such strain fields interact, the structure may become unstable, and hence the extent of such substitutions will be limited. It would be of interest to examine this issue for (Ca,Sr) solid-solution in these structure types by synthesis, and characterize the relation between the compositions of the nascent solutions and the compositions of the crystallizing phases.

Figure 9 shows a type-II stability diagram (Shannon & Prewitt 1970) for these three structure-types. For the phosphates, the separation into two distinct fields is quite marked: minerals of the fairfieldite group contain

(relatively) large ($> 0.76 \text{ \AA}$) octahedrally coordinated cations (Fe^{2+} , Mn^{2+}), whereas phosphate minerals of the collinsite group contain (relatively) small ($< 0.76 \text{ \AA}$) octahedrally coordinated cations (Ni, Mg, Co^{2+} , Zn). For the arsenates, the situation is quite different: all compositions of arsenates ($M^{2+} = Mg, Zn, Co, Mn$) are dimorphous and crystallize in both the brandtite- and collinsite-type structures. Inspection of the structures of these minerals (Figs. 1, 5) shows no obvious constraints on the sizes of the tetrahedra and octahedra within the structural unit itself.

We are unable to come up with a convincing explanation of the findings displayed in Figure 9 (*cf.* Keller *et al.* 2004, Kolitsch & Fleck 2005). However, we note that as the polyhedra link *via* corners, and as there are no linkages that could be affected by articulation requirements between polyhedra, *these constraints on cation size must arise from linkage between structural units* (*i.e.*, either hydrogen bonds or Ca–O bonds).

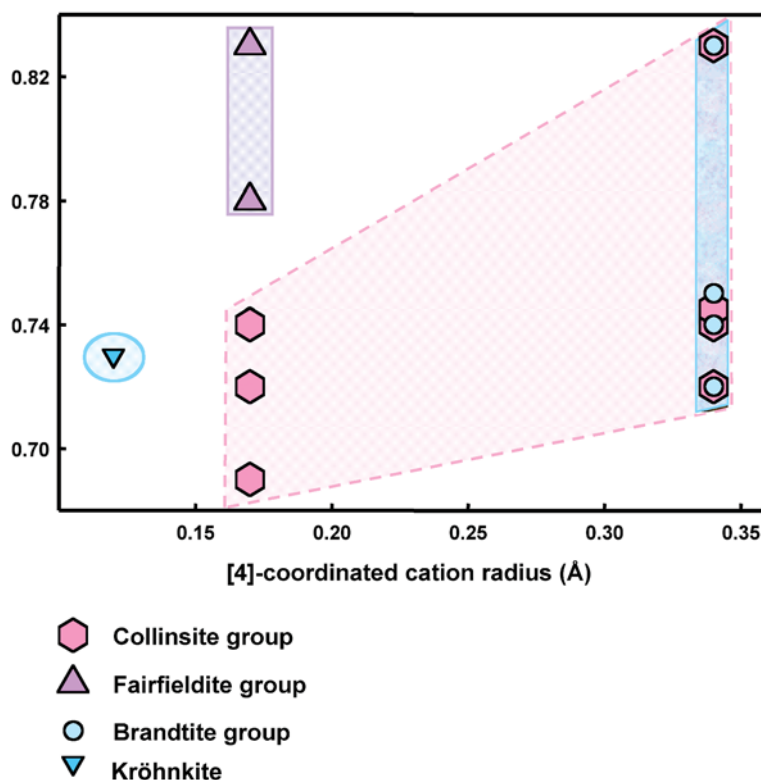


FIG. 9. Type-II stability diagram for the $Ca_2[M(TO_4)_2(H_2O)_2]$ minerals; the fields of the brandtite- (circles), collinsite- (hexagons) and fairfieldite-group (triangles) structures are shown in blue, pink and mauve, respectively.

SYNTHETIC PHASES OF COMPOSITION
 $X_2Y(TO_4)_2(H_2O)_2$

Recently, there has been a considerable amount of work on a wide range of synthetic phases of general composition $X_2Y(TO_4)_2(H_2O)_2$ (Fleck & Kolitsch 2003, Fleck *et al.* 2002a, b, Kolitsch & Fleck 2005, Wildner & Stoilova 2003). In particular, Fleck *et al.* (2002b) introduced a classification of structures based on the $[Y(TO_4)_2(H_2O)_2]$ (kröhnkite-type) chain, dividing the over 50 compounds with this structural motif into six different types labeled A to F on the basis of “differences concerning their linkage to layers as well as the stacking of the layers”. The brandtite, collinsite and fairfieldite groups correspond to the type-D, -A and -B structures, respectively, in this classification.

Hydrogen bonding in the type-C structure

The type-C structure corresponds to $X = K$, $Y = Mn^{2+}$, Cd , $T = S$, Se (Peytavin *et al.* 1974, Fleck *et al.* 2002a). In this structure type, the space group is $P\bar{1}$, and the cell volume has approximately twice the cell volume of the collinsite and fairfieldite structures, and hence $Z = 2$. Thus there are two crystallographically distinct (H_2O) groups in the type-C structure, as distinct from one in the brandtite-, collinsite- and fairfieldite-

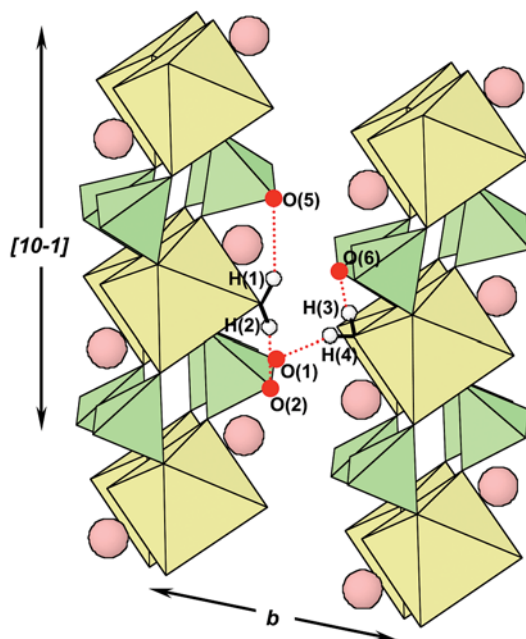


FIG. 10. The crystal structure of $K_2Mn^{2+}(SO_4)_2(H_2O)_2$, a type-C structure showing the disposition of the hydrogen bonds. Legend as in Figure 1.

group structures. The hydrogen-bonding arrangement is shown in Figure 10, where it is immediately apparent that the two crystallographically distinct (H_2O) groups have different schemes of hydrogen bonding. The hydrogen bonds involving the H(1) and H(2) atoms have both acceptor O(4) anions in the same chain as the donor anion, a feature that does not occur in the brandtite, collinsite and fairfieldite structures (*cf.* Figs. 1, 10). The hydrogen bonds involving the H(3) and H(4) atoms are also of different character from those in the brandtite, collinsite and fairfieldite structures in that both H(3) and H(4) bond to O(3) anions of different chains (Fig. 10).

*Symmetrical hydrogen-bonding
 in $KFe^{2+}H(SO_4)_2(H_2O)_2$*

Fleck *et al.* (2002a) showed that the H atom not associated with the (H_2O) group in this (type-E) structure forms a symmetrical hydrogen bond (see also Macíček *et al.* 1994). Symmetrical hydrogen-bonds are not common, and it always is of interest to understand why they occur where they do. As is usually the case, the reason for the symmetrical hydrogen-bond is found in the details of the bond topology of the structure. To see this, it is instructive to compare the structures of $KFe^{2+}H(SO_4)_2(H_2O)_2$ (a type-E structure, Fig. 11) and $K_2Mn^{2+}(SO_4)_2(H_2O)_2$ (a type-C structure) in terms of their bond-valence arrangements; this is done in Table 9. Omitting the H(3) atom, the sum of the bond valence incident at the O(1) site in the type-E structure is 1.50 *vu*. The attitude of adjacent chains is such that O(1) atoms of adjacent chains oppose each other at a distance of 2.47 Å. Each O(1) atom requires an additional 0.50 *vu* to satisfy the valence-sum rule, and with a coordination number of [2], a central H(3) atom satisfies this requirement. However, the potential experienced by a hydrogen atom in this position is of the double-well type, and the H atom usually occupies an off-center position in accord with this. Where in this off-center position, the incident bond-valence sums incident at the two coordinating O atoms are ~2.3 and ~1.7 *vu*, respectively, deviating significantly from the valence-sum rule; thus there is a tendency for the H atom to move away from the former O-atom toward the latter O-atom. Where in the alternate arrangement, the bond-valence sums are reversed, ~1.7 and ~2.3 *vu*, respectively, and the H atom moves in the reverse direction. This argument suggests that the “central” H-atom actually hops between the two asymmetric positions, and two centers of electron density are seen on the time-scale of the diffraction experiment. This mechanism is in accord with the results of Fleck *et al.* (2002a), who observed two electron-density maxima between the O(1) atoms at both room temperature and 110 K.

Further inspection of the bond-valence table for $KFe^{2+}H(SO_4)_2(H_2O)_2$ (Table 9) shows incident bond-valence sums of 2.31 and 1.89 *vu* around the O(3) and

O(4) anions. Note that according to Table 9, the O(3) anion receives hydrogen bonds from both H(1) and H(2), whereas the O(4) anion receives no hydrogen bonds at all. If both O(3) and O(4) each received one hydrogen-bond, the analogous bond-valence sums would be 2.11 and 2.09 *vu*, respectively. The corresponding H(1)–O(4) distance is 2.50 Å, and the OW–H(1)...O(4) angle is 120°. The former distance is fairly long for a hydrogen bond, but Brown (1976) has shown that H...O interactions in the range 2.3–3.1 Å are significant (in perchloric acid hydrates). Moreover, such long H...O distances in perchloric acid hydrates involve O–H...O angles of 80–120°, in accord with the OW–H(1)...O(4) angle of 120° found here. Thus bond valences suggest a hydrogen-bond arrangement in $\text{KFe}^{2+}\text{H}(\text{SO}_4)_2(\text{H}_2\text{O})_2$ different from that currently proposed.

ACKNOWLEDGEMENTS

We thank reviewers M. Fleck, G. Ferraris and Associate Editor Uwe Kolitsch for their comments. This work was supported by a Canada Research Chair in Crystallography and Mineralogy, Research Tools and Equipment, Major Facilities Access and Discovery Grants from the Natural Sciences and Engineering Research Council of Canada and Canada Foundation for Innovation Grants to FCH.

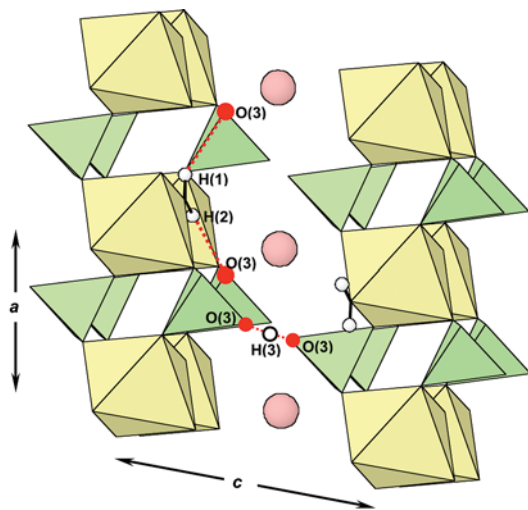


FIG. 11. The crystal structure of $\text{KFe}^{2+}\text{H}(\text{SO}_4)_2(\text{H}_2\text{O})_2$, a type-C structure, projected onto (010). Legend as in Figure 1. Note that the H(3) site is placed at the average of the two half-occupied (symmetry-related) positions to emphasize the symmetrical nature of the hydrogen bond.

TABLE 9. BOND-VALENCE (*vu*)^{*} TABLES FOR TYPE-C AND TYPE-E STRUCTURES

Type C: $\text{K}_2\text{Mn}^{2+}(\text{SO}_4)_2(\text{H}_2\text{O})_2$										
	K(1)	K(2)	Mn ²⁺	S(1)	S(2)	H(1)	H(2)	H(3)	H(4)	Σ
O(1)	0.10	0.15		1.56					0.20	2.01
O(2)		0.18		1.50			0.20			2.05
		0.17								
O(3)		0.18	0.36	1.45						1.99
O(4)	0.19	0.15	0.32	1.43						2.09
O(5)	0.12				1.53	0.20				2.03
	0.18									
O(6)	0.15				1.52			0.20		1.87
O(7)	0.10		0.32		1.44					1.97
	0.11									
O(8)	0.15	0.14	0.36		1.44					2.09
O(9)	0.14		0.33			0.80	0.80			2.07
O(10)		0.12	0.37					0.80	0.80	2.09
Σ	1.24	1.09	2.06	5.94	5.93	1.0	1.0	1.0	1.0	

Type E: $\text{K}_2\text{Fe}^{2+}\text{H}(\text{SO}_4)_2(\text{H}_2\text{O})_2$										
	K	Fe ²⁺	S	H(1)	H(2)	Σ	H(3)	Σ		
O(1)		0.08 ^{o2} ; 0.07 ^{o2} ;	1.35			1.50	0.50 ^{o2} ;	2.00		
O(2)		0.19 ^{o2} ;	0.35 ^{o2} ;	1.52				2.06		
O(3)		0.16 ^{o2} ;		1.59	0.2	0.2		2.31		
O(4)			0.37 ^{o2} ;	1.52				1.89		
O(5)		0.05 ^{o2} ;	0.34 ^{o2} ;		0.8	0.8		1.99		
Σ	1.10	2.12	5.98	1.0	1.0		1.00			

* O(1) is involved in a very short (symmetrical) hydrogen-bond.

REFERENCES

- BROTHERTON, P.D., MASLEN, E.N., PRYCE, M.W. & WHITE, A.H. (1974): Crystal structure of collinsite. *Aust. J. Chem.* **27**, 653-656.
- BROWN, I.D. (1976): Hydrogen bonding in perchloric acid hydrates. *Acta Crystallogr.* **A32**, 786-792.
- BROWN, I.D. (1981): The bond-valence method: an empirical approach to chemical structure and bonding. *In Structure and Bonding in Crystals II* (M. O'Keeffe & A. Navrotsky, eds.). Academic Press, New York, N.Y. (1-30).
- BROWN, I.D. & ALTERMATT, D. (1985): Bond-valence parameters obtained from a systematic analysis of the inorganic crystal structure database. *Acta Crystallogr.* **B41**, 244-247.
- BURNS, P.C. (1999): The crystal chemistry of uranium. *In Uranium: Mineralogy, Geochemistry and the Environment* (P.C. Burns & R. Finch, eds.). *Rev. Mineral.* **38**, 23-90.
- BURNS, P.C., MILLER, M.L. & EWING, R.C. (1996): U⁶⁺ minerals and inorganic phases: a comparison and hierarchy of structure. *Can. Mineral.* **34**, 845-880.
- CATTI, M., FERRARIS, G. & IVALDI, G. (1977): Hydrogen bonding in the crystalline state. Structure of talmesite, $\text{Ca}_2(\text{Mg},\text{Co})(\text{AsO}_4)_2 \cdot 2\text{H}_2\text{O}$, and crystal chemistry of

- related minerals. *Bull. Soc. Fr. Minéral. Crystallogr.* **100**, 230-236.
- DAHLMAN, B. (1951): The crystal structures of kröhnkite, $\text{CuNa}_2(\text{SO}_4)_2 \cdot 2\text{H}_2\text{O}$ and brandtite, $\text{MnCa}_2(\text{AsO}_4)_2 \cdot 2\text{H}_2\text{O}$. *Arkiv Mineral. Geol.* **1**, 339-366.
- DUNN, P.J., PEACOR, D.R., SU, SHU-CHUN, WICKS, F.J. & PARKER, F.J. (1987b): Parabrandtite, the manganese analogue of talnessite, from Sterling Hill, Ogdensburg, New Jersey. *Neues Jahrb. Mineral., Abh.* **157**, 113-119.
- DUNN, P.J., STURMAN, D.B. & NELEN, J.A. (1987a): Wendwilsonite, the Mg analogue of roselite, from Morocco, New Jersey, and Mexico, and new data on roselite. *Am. Mineral.* **72**, 217-221.
- FANFANI, L., NUNZI, A. & ZANAZZI, P.F. (1970): The crystal structure of fairfieldite. *Acta Crystallogr.* **B26**, 640-645.
- FLECK, M. & KOLITSCH, U. (2003): Natural and synthetic compounds with kröhnkite-type chains; an update. *Z. Kristallogr.* **218**, 553-567.
- FLECK, M., KOLITSCH, U. & HERTWECK, B. (2002b): Natural and synthetic compounds with kröhnkite-type chains: review and classification. *Z. Kristallogr.* **217**, 435-443.
- FRONDEL, C. (1955): Neomesselite and beta-roselite: two new members of the fairfieldite group. *Am. Mineral.* **40**, 828-833.
- HAWTHORNE, F.C. (1983): Graphical enumeration of polyhedral clusters. *Acta Crystallogr.* **A39**, 724-736.
- HAWTHORNE, F.C. (1984): The crystal structure of stononite and the classification of the alumino-fluoride minerals. *Can. Mineral.* **22**, 245-251.
- HAWTHORNE, F.C. (1985): Towards a structural classification of minerals: the $^{\text{VI}}\text{M}^{\text{IV}}\text{T}_2\phi_n$ minerals. *Am. Mineral.* **70**, 455-473.
- HAWTHORNE, F.C. (1986): Structural hierarchy in $^{\text{VI}}\text{M}_x^{\text{III}}\text{T}_y\phi_z$ minerals. *Can. Mineral.* **24**, 625-642.
- HAWTHORNE, F.C. (1990): Structural hierarchy in $\text{M}^{[\text{VI}]\text{T}^{[\text{IV}]}}\phi_n$ minerals. *Z. Kristallogr.* **192**, 1-52.
- HAWTHORNE, F.C. (1992): Bond topology, bond-valence and structure stability. In *The Stability of Minerals* (G.D. Price & N.L. Ross, eds.). Chapman & Hall, London, U.K. (25-87).
- HAWTHORNE, F.C. (1994): Structural aspects of oxides and oxysalt crystals. *Acta Crystallogr.* **B50**, 481-510.
- HAWTHORNE, F.C. (1997): Structural aspects of oxide and oxysalt minerals. In *Modular Aspects of Minerals* (S. Merlino, ed.). *Eur. Mineral. Union, Notes in Mineralogy* **1**, 373-429.
- HAWTHORNE, F.C., BURNS, P.C. & GRICE, J.D. (1996): The crystal chemistry of boron. In *Boron: Mineralogy, Petrology and Geochemistry* (E.S. Grew & L.M. Anovitz, eds.). *Rev. Mineral.* **33**, 41-115.
- HAWTHORNE, F.C. & FERGUSON, R.B. (1975): Refinement of the crystal structure of kröhnkite. *Acta Crystallogr.* **B31**, 1753-1755.
- HAWTHORNE, F.C. & FERGUSON, R.B. (1977): The crystal structure of roselite. *Can. Mineral.* **15**, 36-42.
- HAWTHORNE, F.C. & HUMINICKI, D.M.C. (2002): The crystal chemistry of beryllium. In *Beryllium: Mineralogy, Petrology, and Geochemistry* (E.S. Grew, ed.). *Rev. Mineral. Geochem.* **50**, 333-403.
- HAWTHORNE, F.C., KRIVOVICHEV, S.V. & BURNS, P.C. (2000): The crystal chemistry of sulfate minerals. In *Sulfate Minerals – Crystallography, Geochemistry, and Environmental Significance* (C.N. Alpers, J.L. Jambor & D.K. Nordstrom, eds.). *Rev. Mineral. Geochem.* **40**, 1-112.
- HAWTHORNE, F.C., UNGARETTI, L. & OBERTI, R. (1995): Site populations in minerals: terminology and presentation of results of crystal-structure refinement. *Can. Mineral.* **33**, 907-911.
- HEJNY, C., GIESTER, G., WILDNER, M. & GÖTZINGER, M. (1997): Die Kristallstruktur von Brandtit, $\text{Ca}_2\text{Mn}(\text{AsO}_4)_2 \cdot 2\text{H}_2\text{O}$. *Ber. Deutsch. Mineral. Gesellschaft, Beih.* **1**, 150 (abstr.).
- HUMINICKI, D.M.C. & HAWTHORNE, F.C. (2002): The crystal chemistry of the phosphate minerals. In *Phosphates: Geochemical, Geobiological, and Materials Importance* (M.L. Kohn, J. Rakovan & J.M. Hughes, eds.). *Rev. Mineral. Geochem.* **48**, 123-253.
- JOSWIG, W., PAULUS, E.F. & LIEBSCHER, B. (2004): Crystal structure of dicalcium (cobalt,magnesium) diarsenate dihydrate, $\text{Ca}_2(\text{Co}_{0.532}\text{Mg}_{0.468})[\text{AsO}_4]_2 \cdot 2\text{H}_2\text{O}$, hydrogen bonding in talnessite. *Z. Kristallogr.* **219**, 341-342.
- KELLER, P., INNES, J. & DUNN, P.J. (1986): Zincroselite, $\text{Ca}_2\text{Zn}(\text{AsO}_4)_2(\text{H}_2\text{O})_2$, a new mineral from Tsumeb, Namibia. *Neues Jahrb. Mineral., Monatsh.*, 523-527.
- KELLER, P., LISSNER, F. & SCHLEID, T. (2002): Zinkroselith und Gaitit, zwei Modifikationen von $\text{Ca}_2\text{Zn}(\text{AsO}_4)_2 \cdot 2\text{H}_2\text{O}$, aus Tsumeb (Namibia). *Z. Kristallogr., Suppl.* **19**, 87.
- KELLER, P., LISSNER, F. & SCHLEID, T. (2004): The crystal structures of zincroselite and gaitite: two natural polymorphs of $\text{Ca}_2\text{Zn}[\text{AsO}_4]_2 \cdot 2\text{H}_2\text{O}$ from Tsumeb, Namibia. *Eur. J. Mineral.* **16**, 353-359.
- KOLITSCH, U. & FLECK, M. (2005): Second update on compounds with kröhnkite-type chains. *Z. Kristallogr.* **220**, 31-41.
- LIEBAU, F. (1985): *Structural Chemistry of Silicates: Structure, Bonding, and Classification*. Springer-Verlag, Berlin, Germany.
- LIFEROVICH, R.P., PAKHOMOVSKY, YA.A., BOGDANOVA, A.N., BALAGANSKAYA, E.G., LAAJOKI, K.V.O., GEHÖR, S. &

- CHUKANOV, N.V. (2001): Collinsite in hydrothermal assemblages related to carbonatites in the Kovdor complex, northwestern Russia. *Can. Mineral.* **39**, 1081-1094.
- MACÍČEK, J., GRADINAROV, S., BONTCHEV, R. & BALAREW, C. (1994): A short dynamically symmetrical hydrogen bond in the structure of $K(Mg(H_{0.5}SO_4)_2(H_2O)_2)$. *Acta Crystallogr.* **C50**, 1185-1188.
- PEYTAVIN, S., AVINENS, C., COT, L. & MAURIN, M. (1974): Structural systematics of divalent tetrahedral anionic compounds having the formula $M^I_2M^{II}(AB_4)_2 \cdot H_2O$. *Rev. Chim. Minérale* **11**, 689-700.
- SABELLI, C. & TROSTI-FERRONI, R. (1985): A structural classification of sulfate minerals. *Per. Mineral.* **54**, 1-46.
- SHANNON, R.D. & PREWITT, C.T. (1970): Effective ionic radii and crystal chemistry. *J. Inorg. Nucl. Chem.* **32**, 1427-1441.
- STURMAN, D.B. & DUNN, P.J. (1980): Gaitite, $H_2Ca_2Zn(AsO_4)_2(OH)_2$, a new mineral from Tsumeb, Namibia (Southwest Africa). *Can. Mineral.* **18**, 197-200.
- WILDNER, M. & STOILOVA, D. (2003): Crystal structures and crystal chemical relationships of kröhnkite- and collinsite-type compounds $Na_2Me^{2+}(XO_4)_2 \cdot 2H_2O$ ($X = S, Me = Mn, Cd$; and $X = Se, Me = Mn, Co, Ni, Zn, Cd$) and $K_2Co(SeO_4)_2 \cdot 2H_2O$. *Z. Kristallogr.* **218**, 201-209.
- YAKUBOVICH, O.V., MASSA, W., LIFEROVICH, R.P., GAVRILENKO, P.G., BOGDANOVA, A.N. & TUISKU, P. (2003): Hillite, a new member of the fairfieldite group: its description and crystal structure. *Can. Mineral.* **41**, 981-988.

Received August 31, 2005, revised manuscript accepted March 6, 2006.